Numerical analysis of pressure gradients in piping due to hydraulic transients to determine critical axial loads

Rodrigo B. Rabelo[1], Ivan F. M. Menezes[2], Luis F. G. Pires[3]

[1] *Dept. of Pipeline Engineering, Petrobras*
Av. Henrique Valadares, 28, 20231-030, Rio de Janeiro/RJ, Brazil
rodrigobr@petrobras.com.br
[2]*Dept. of Mechanical Engineering, PUC-Rio*
Rua Marquês de São Vicente, 225, Prédio Cardeal Leme, 22453-900, Rio de Janeiro/RJ, Brazil
ivan@puc-rio.br
[3]*SIMDUT, PUC-Rio*
Rua Marquês de São Vicente, 225 Prédio Pe Laércio Dias de Moura, 22451-900, Rio de Janeiro/RJ, Brazil
lpires@esp.puc-rio.br

Abstract. Hydraulic transient or "water hammer" is the sudden pressure variation in a fluid system. In pipelines, it is often associated with closing valves and starting and stopping pumps. In aerial installations, it may produce great axial forces due to the steep pressure differentials that may occur. To correctly dimension pipe supports, stress analysis studies must consider these loads, which, in turn, require hydraulic simulations. Often this data is unavailable given the required deadlines. The work presented here aims to provide data on dynamic forces generated in hydraulic transients in a wide range of cases found in the oil industry. Hydraulic simulations were performed considering various pipeline diameters, flow velocities, and different fluids, analyzing the rapid closure of a ball valve. These simulations provided the pressure gradients that occur across multiple pipe lengths. Quadratic interpolations were then performed with the data obtained by the simulations, and it was verified that they were adequate to get pressure gradients for scenarios of flow velocities and density values intermediate to those of the simulated cases without the need to carry out new simulations. It was also verified that a fifth-order polynomial could perfectly describe the pressure gradient curves of each scenario, allowing the results to be obtained by simple equations.

Keywords: hydraulic transients, hydraulic simulation, pressure gradients, dynamic loads in piping.

1 Introduction

Hydraulic transient or "water hammer" is the sudden variation of pressure in a fluid system caused by a change of flow that occurs over a relatively short period. In pipelines, it is often associated with the closing/opening of a valve or starting/stopping of pumps. Hydraulic transients may generate pressure values much higher than the ones in regular operation. In aerial installations, hydraulic transients may produce great axial forces due to the steep pressure differentials that may arise just after the beginning of the surge, before line packing occurs. To properly dimension pipe supports, the Stress Analysis studies must consider these loads. The Energy Institute [1] provides an estimate for these loads for some situations based on the Joukowsky equation but also states that, for a detailed surge analysis, hydraulic simulations are required. Often this data is unavailable, given the necessary demand and deadline.

In this scenario, the work presented in this paper aimed to provide data on dynamic forces generated in hydraulic transients in a wide range of cases found in the oil industry.

It started with performing hydraulic simulations considering various pipeline diameters, flow rates, and transported products, analyzing the rapid closure of a valve, and obtaining the pressure gradients that occur across multiple pipe lengths. After all the simulations, an attempt was made to obtain a correlation between the data so that pressure gradients could be obtained in intermediate cases of flow velocity or density of the fluid.

The results of this work are shown next.

2 Study conception and input data

2.1 Concept of "pressure gradient"

During a water hammer, the pressure changes propagate with the sound wave speed in the fluid/pipe system. As the pressure wave moves, the pressure slope along the distance is reduced due to the attenuation. As stated by Chaudhry [2], that occurs because the velocity differential across the wavefront is reduced as the wave propagates in the upstream direction, and also due to friction losses. Therefore, although the pressure differential (in absolute values) in a given pipe length will be greater with the increase in the extension of the piping, the "effective slope" of the pressure with respect to the distance is more significant in small sections, reducing as a greater length is considered.

This paper uses the term "pressure gradient" to describe the "effective" pressure slope that produces the pressure differential observed in an evaluated pipeline/piping extension. Figure 1 illustrates what was discussed above, showing the pressure profile in a pipeline during a water hammer, in a selected time step. The pressure differential in a given piping length will produce a force, that must be withstood by piping supports.

The pressure differential in piping segment L_2 (greater length) is greater than the pressure differential that occurs in segment L_1. But the pressure gradient (the "effective" pressure slope) is more significant in the smaller piping (L_1).

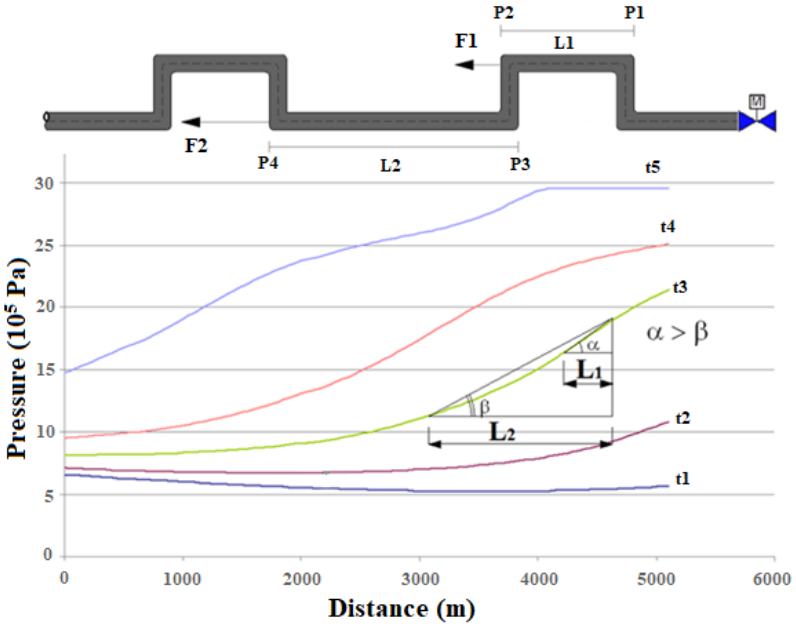

Figure 1. Pressure profile during water hammer and "effective" pressure slopes in piping lengths

2.2 Studied cases

This work aims to obtain the most critical pressure gradients that occur during the hydraulic transient of the quick closing of a valve, for several pipe sections, for a wide range of cases typical in the oil industry. Thus, hydraulic simulations were performed considering the following cases:

- Pipeline Nominal Diameters (DN) from 250 to 600
- Fluids simulated: gasoline, diesel, and LCO (light cracking oil)
- Flow velocity: 1m/s, 2m/s and 3m/s

All cases constitute a total of 72 simulations.

It was considered the closing of a ball valve in 5 seconds. It was used a real valve closing curve and valve coefficient C_v, provided by Cameron [3 and 4]. Figure 2 presents the valve curve and the values of C_v considered for each pipe diameter. Table 1 presents the properties considered for each fluid simulated. The density was obtained from Safety Data Sheet for Chemical Products (FISPQ) from Petrobras [5, 6 and 7]. The bulk modulus was calculated using the API Manual of Petroleum Measurement Standards, Chapter 11.2.1 [8].

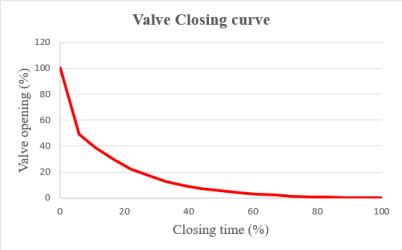

Valve diameter	Cv ($m^3/s.MPa^{0.5}$)
DN 250	13.07
DN 300	19.69
DN 350	23.50
DN 400	32.33
DN 450	42.68
DN 500	54.58
DN 550	67.25
DN 600	83.11

Figure 2. Valve closing curves and C_v values

Table 1. Fluid properties

Fluid	Density (kg/m^3)	Viscosity (cP)	Bulk modulus (GPa)
Gasoline	770	0.41	1.04
Diesel	880	2.2	1.51
LCO	980	2.45	1.91

To perform the hydraulic simulations, the software Synergi Pipeline Simulator from DNV was used. The system elaborated for the simulation is illustrated in Fig. 3. A 50 km pipeline and a 1 km piping were considered. The long pipeline was modeled to avoid the damping of the pressure gradient due to the reflection of the wave (Brandt et al. [9]). Piping was divided into 10 m segments.

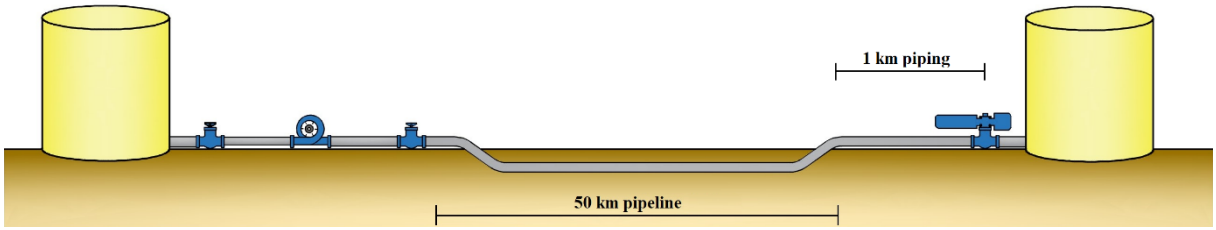

Figure 3. System simulated

It was adopted a knot spacing of 5 m. Once resistance to flow is relatively small in the initial stages of closure (Jones et al. [10]), a computational code was written so that during the last moments of valve closing, the time step was forced to remain near the minimum value defined by the software.

After performing each simulation case, the critical pressure gradients through the 1 km piping were obtained from the pressure values at the ends of each of the 10 m pipe segments following the methodology suggested by Correia and Rabelo [11]. The pressure differential between these points was calculated for each time step, and the maximum value was selected. This process was repeated for different pipe lengths, from 10 m to 500 m, and thus the critical pressure gradient for each of these pipe lengths was obtained.

3 Simulation results

The pressure gradients for gasoline, diesel, and LCO are presented respectively in Figs. 4, 5, and 6. The pressure gradients were obtained for pipe lengths from 10 m to 500 m for the hydraulic transient of a ball valve closing in 5 seconds for the flow velocities of 1 m/s, 2 m/s, and 3 m/s. For convenience in representing the values, the unit "10^2 Pa/m" or "hPa/m" was adopted for the pressure gradients.

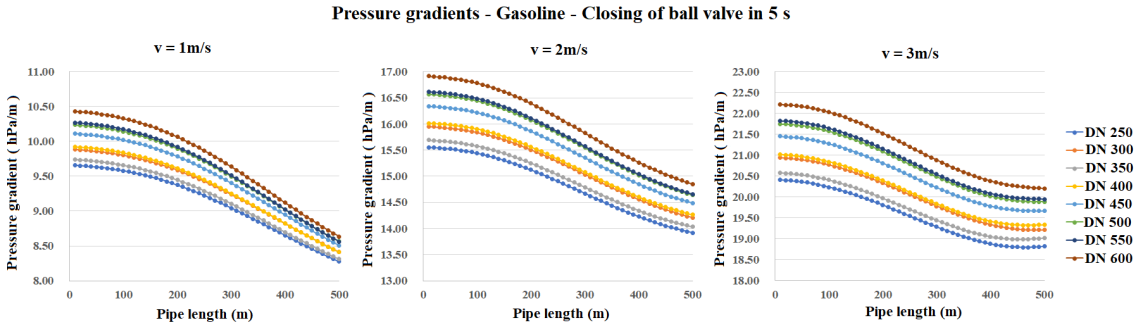

Figure 4. Pressure gradients for gasoline

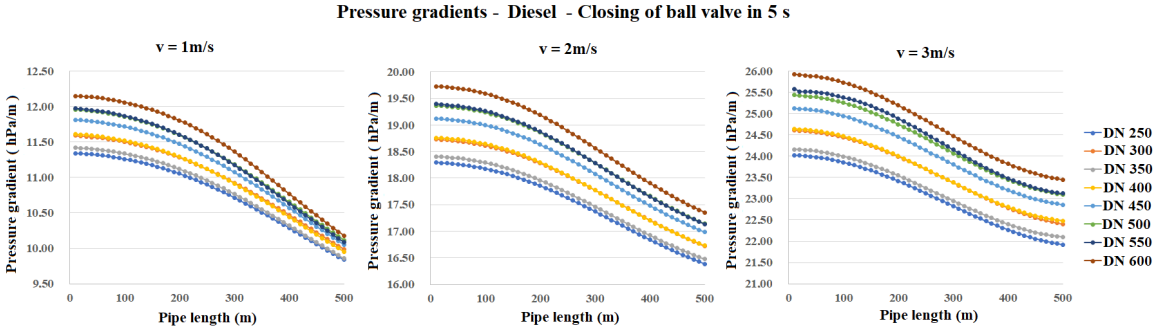

Figure 5. Pressure gradients for diesel

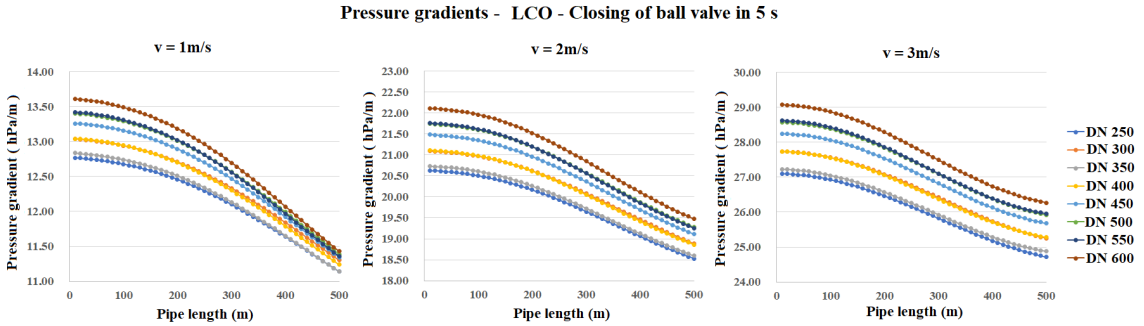

Figure 6. Pressure Gradients for LCO

The results show curves where the pressure gradient is higher for small pipe sections, decreasing with the increase of the pipe length in which the gradient is evaluated. As commented in section 2.1, this behavior is expected and can be explained by the attenuation of the pressure wave. It is again highlighted that the pressure differential in a larger piping section will be higher; it is the pressure gradient that will be reduced.

The pressure gradients show similar behavior for all simulated diameters, with a tendency for numerical values to increase with increasing diameter. The exception was the case of the DN 350 piping, which presented slightly smaller gradients than the case of the DN 300.

The results show greater numerical values of the gradients of diesel compared to gasoline, and greater values for LCO compared to the other liquids. These results were expected due to the higher density and Bulk Modulus of the fluids.

4 Data analysis and correlations

Having obtained the pressure gradients for gasoline, diesel, and LCO, at flow velocities of 1 m/s, 2 m/s, and

3 m/s, the objective becomes to analyze the data produced in search of a correlation that allows the determination of pressure gradients to other values of velocity and density without the need to perform new hydraulic simulations.

4.1 Flow velocities correlation

Using the LCO simulation data, quadratic interpolations were performed between the velocity results for each pipe length from 10m to 500m in order to obtain pressure gradients for any value between 1 m/s and 3 m/s.

To verify if the pressure gradients obtained by quadratic interpolation are adequate, hydraulic simulations of the closing of the ball valve were performed, considering the flow of LCO at velocities of 1.5 m/s and 2.5 m/s. The maximum relative error of the quadratic interpolation was 0.328% for a flow velocity of 1.5 m/s and 0.329% for a velocity of 2.5 m/s. Therefore, there is good evidence that quadratic interpolation is adequate for obtaining pressure gradients for any velocity value between 1 and 3 m/s without requiring new hydraulic simulations.

The quadratic interpolation was also performed for gasoline and diesel, for all pipe diameters between DN 250 to DN 600. Figure 7 presents the pressure gradients for several flow velocities, for the flow of LCO and a DN 600 pipeline.

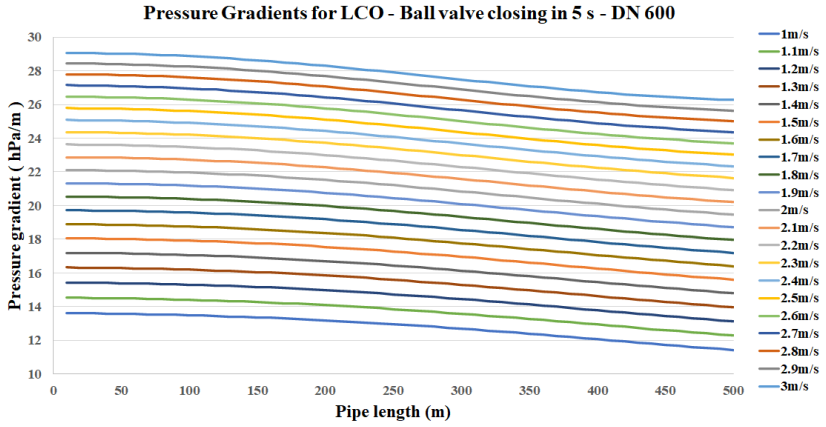

Figure 7. Pressure gradients for LCO – DN 600

4.2 Density correlation

Similar to what was done in the previous section, quadratic interpolations were performed, for each simulated pipe diameter and flow velocity, to obtain the pressure gradients for different densities between 770 and 980 kg/m³. Figure 8 presents the pressure gradients for a DN 600 pipeline and a 3 m/s flow velocity for several densities.

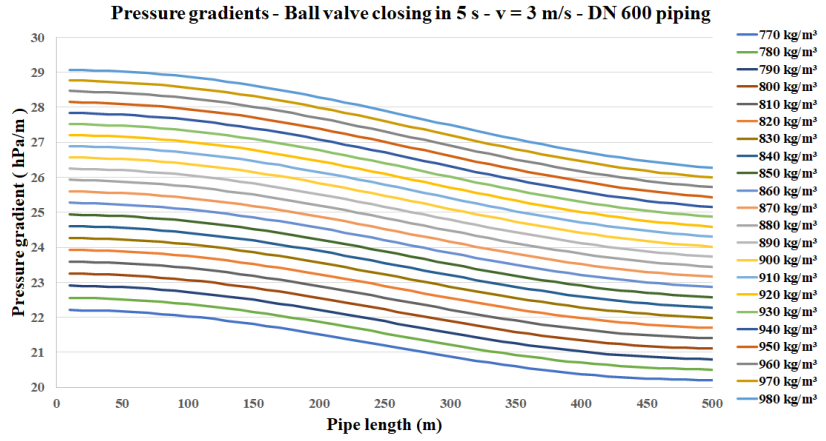

Figure 8. Pressure gradients for DN 600 piping and 3 m/s flow velocity

4.3 Combined correlation of velocity and density

During the analysis of the simulation results for different density values, it was observed that a linear interpolation would almost be enough to interconnect the results for gasoline, diesel, and LCO.

Figure 9 illustrates a proposal to condense the information from several graphs into one. It was based on the results of pressure gradients for diesel. The values were divided by the specific gravity "SG" of the fluid, to be applied to hydrocarbons with specific gravity between 0.77 and 0.98 (density between 770 kg/m³ and 980 kg/m³). Therefore, this proposal provides pressure gradients for cases where both the flow velocity and the density are intermediate values of those simulated. The maximum relative error of the graph is 3.32% near the density of 770 kg/m³ and 0.85% near the density of 880 kg/m³. The results in Figure 9 correspond to a DN 600 pipeline.

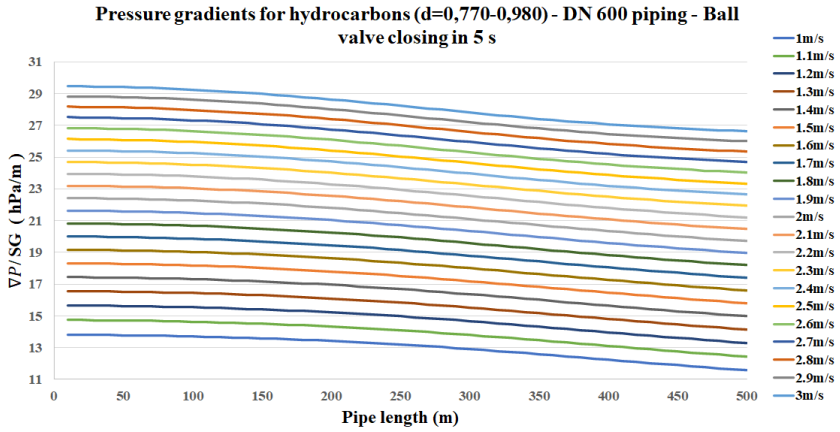

Figure 9. Pressure gradients for DN 600 piping

It was verified that a fifth-order polynomial could perfectly describe the pressure gradient curves produced, with a coefficient of determination $R^2 = 1$ in all cases. Therefore, the results of the pressure gradients shown in the figures can be obtained by simple equations.

The following equations provide the pressure gradients shown in Figure 9, where "x" is the piping length being evaluated.

1m/s: $\frac{\nabla P}{sg} = 4.0464\ 10^{-14}x^5 - 5.9936\ 10^{-12}x^4 - 1.2768\ 10^{-8}x^3 - 5.2533\ 10^{-6}x^2 - 4.4831\ 10^{-4}x + 13.816.$ (1)

1.1m/s: $\frac{\nabla P}{sg} = 1.6691\ 10^{-14}x^5 + 2.1541\ 10^{-11}x^4 - 2.2026\ 10^{-8}x^3 - 4.7124\ 10^{-6}x^2 - 4.8465\ 10^{-4}x + 14.748.$ (2)

1.2m/s: $\frac{\nabla P}{sg} = -5.5522\ 10^{-15}x^5 + 4.7236\ 10^{-11}x^4 - 3.0518\ 10^{-8}x^3 - 4.2805\ 10^{-6}x^2 - 5.1659\ 10^{-4}x + 15.664.$ (3)

1.3m/s: $\frac{\nabla P}{sg} = -2.6266\ 10^{-14}x^5 + 7.1094\ 10^{-11}x^4 - 3.8244\ 10^{-8}x^3 - 3.9578\ 10^{-6}x^2 - 5.4413\ 10^{-4}x + 16.565.$ (4)

1.4m/s: $\frac{\nabla P}{sg} = -4.5449\ 10^{-14}x^5 + 9.3113\ 10^{-11}x^4 - 4.5206\ 10^{-8}x^3 - 3.7441\ 10^{-6}x^2 - 5.6728\ 10^{-4}x + 17.449.$ (5)

1.5m/s: $\frac{\nabla P}{sg} = -6.3103\ 10^{-14}x^5 + 1.1329\ 10^{-10}x^4 - 5.1402\ 10^{-8}x^3 - 3.6395\ 10^{-6}x^2 - 5.8603\ 10^{-4}x + 18.318.$ (6)

1.6m/s: $\frac{\nabla P}{sg} = -7.9228\ 10^{-14}x^5 + 1.3164\ 10^{-10}x^4 - 5.6833\ 10^{-8}x^3 - 3.6439\ 10^{-6}x^2 - 6.0038\ 10^{-4}x + 19.172.$ (7)

1.7m/s: $\frac{\nabla P}{sg} = -9.3823\ 10^{-14}x^5 + 1.4814\ 10^{-10}x^4 - 6.1498\ 10^{-8}x^3 - 3.7574\ 10^{-6}x^2 - 6.1034\ 10^{-4}x + 20.009.$ (8)

1.8m/s: $\frac{\nabla P}{sg} = -1.0689\ 10^{-13}x^5 + 1.6281\ 10^{-10}x^4 - 6.5398\ 10^{-8}x^3 - 3.9801\ 10^{-6}x^2 - 6.1590\ 10^{-4}x + 20.831.$ (9)

1.9m/s: $\frac{\nabla P}{sg} = -1.1842\ 10^{-13}x^5 + 1.7563\ 10^{-10}x^4 - 6.8533\ 10^{-8}x^3 - 4.3117\ 10^{-6}x^2 - 6.1706\ 10^{-4}x + 21.637.$ (10)

2m/s: $\frac{\nabla P}{sg} = -1.2843\ 10^{-13}x^5 + 1.8662\ 10^{-10}x^4 - 7.0902\ 10^{-8}x^3 - 4.7525\ 10^{-6}x^2 - 6.1382\ 10^{-4}x + 22.427.$ (11)

2.1m/s: $\frac{\nabla P}{sg} = -1.3690\ 10^{-13}x^5 + 1.9577\ 10^{-10}x^4 - 7.2506\ 10^{-8}x^3 - 5.3023\ 10^{-6}x^2 - 6.0619\ 10^{-4}x + 23.202.$ (12)

2.2m/s: $\frac{\nabla P}{sg} = -1.4385\ 10^{-13}x^5 + 2.0308\ 10^{-10}x^4 - 7.3344\ 10^{-8}x^3 - 5.9612\ 10^{-6}x^2 - 5.9416\ 10^{-4}x + 23.961.$ (13)

2.3m/s: $\frac{\nabla P}{d} = -1.4927\ 10^{-13}x^5 + 2.0856\ 10^{-10}x^4 - 7.3417\ 10^{-8}x^3 - 6.7292\ 10^{-6}x^2 - 5.7773\ 10^{-4}x + 24.704.$ (14)

2.4m/s: $\frac{\nabla P}{sg} = -1.5315\ 10^{-13}x^5 + 2.1219\ 10^{-10}x^4 - 7.2725\ 10^{-8}x^3 - 7.6063\ 10^{-6}x^2 - 5.5691\ 10^{-4}x + 25.432.$ (15)

2.5m/s: $\frac{\nabla P}{sg} = -1.5551\ 10^{-13}x^5 + 2.1399\ 10^{-10}x^4 - 7.1267\ 10^{-8}x^3 - 8.5924\ 10^{-6}x^2 - 5.3169\ 10^{-4}x + 26.144.$ (16)

2.6m/s: $\frac{\nabla P}{sg} = -1.5634\ 10^{-13}x^5 + 2.1395\ 10^{-10}x^4 - 6.9044\ 10^{-8}x^3 - 9.6877\ 10^{-6}x^2 - 5.0207\ 10^{-4}x + 26.840.$ (17)

2.7m/s: $\frac{\nabla P}{d} = -1.5564\ 10^{-13}x^5 + 2.1207\ 10^{-10}x^4 - 6.6056\ 10^{-8}x^3 - 1.0892\ 10^{-5}x^2 - 4.6805\ 10^{-4}x + 27.520.$ (18)

2.8m/s: $\frac{\nabla P}{sg} = -1.5341\ 10^{-13}x^5 + 2.0835\ 10^{-10}x^4 - 6.2302\ 10^{-8}x^3 - 1.2205\ 10^{-5}x^2 - 4.2964\ 10^{-4}x + 28.185.$ (19)

2.9m/s: $\frac{\nabla P}{sg} = -1.4964\ 10^{-13}x^5 + 2.0280\ 10^{-10}x^4 - 5.7783\ 10^{-8}x^3 - 1.3628\ 10^{-5}x^2 - 3.8683\ 10^{-4}x + 28.834.$ (20)

3m/s: $\frac{\nabla P}{sg} = -1.4435\ 10^{-13}x^5 + 1.9540\ 10^{-10}x^4 - 5.2499\ 10^{-8}x^3 - 1.5159\ 10^{-5}x^2 - 3.3963\ 10^{-4}x + 29.467.$ (21)

5 Conclusions

The hydraulic simulations developed in this paper allowed for obtaining pressure gradients for a wide range of cases found in the oil industry.

It was verified that the quadratic interpolation performed with the data produced by the simulations is adequate to obtain pressure gradients for scenarios of flow velocities and density values intermediate to those of the simulated cases without the need to carry out new simulations.

It was also verified that a fifth-order polynomial could perfectly describe the pressure gradient curves of each scenario. Therefore, the results of the pressure gradients shown in the figures can be obtained by simple equations.

The data produced in this work serve as input data for Stress Analysis studies, allowing the adequate design of piping supports to resist the dynamic loads that may occur in the system.

Future work can be developed, considering hydraulic transients of other types of block valves and closing times.

Acknowledgements. The authors acknowledge the technical and financial support from PETROBRAS, CNPq, and Coordenação de Aperfeiçoamento de Pessoal de Nível Superior - Brasil (CAPES) - Finance Code 001.

Authorship statement. The authors hereby confirm that they are the sole liable persons responsible for the authorship of this work, and that all material that has been herein included as part of the present paper is either the property (and authorship) of the authors, or has the permission of the owners to be included here.

References

[1] Energy Institute. *Guidelines for the Avoidance of Vibration Induced Fatigue Failure in Process Pipework*. Energy Institute, 2008.
[2] Chaudhry, M. H. *Applied Hydraulic Transients*. Springer, 2014.
[3] Cameron. *TK Trunnion Mounted Ball Valves*. 2013.
[4] Cameron. *Ball Valve 12" 900# (G23S1) Cv curve*. Provided by e-mail by Cameron.
[5] Petrobras. *Ficha de Informação de Segurança de Produto Químico – FISPQ Gasolina Comum A S50*. 2019.
[6] Petrobras. *Ficha de Informação de Segurança de Produto Químico – FISPQ Óleo Diesel*. 2019.
[7] Petrobras. *Ficha de Informação de Segurança de Produto Químico – FISPQ LCO – Óleo Leve de Craqueamento*. 2019.
[8] American Petroleum Institute, API. *Manual of Petroleum Measurement Standards, MPMS Chapter 11.2.1.* API, 1984.
[9] Brandt, M. J.; Johnson, K. M.; Elphinston, A. J.; Ratnayaka, Don D. *Twort's Water Supply.* Butterworth-Heinemann, 2017.
[10] Jones, G. M.; Sanks, R. L.; Tchobanoglous, G.; Bosserman II, B. E. *Pumping Station Design.* Butterworth-Heinemann, 2008.
[11] Correia, L. C. and Rabelo, R. B. "Methodology for determining the critical pressure differentials using hydraulic simulators for the dynamic analysis of pipelines". In: Instituto Brasileiro do Petróleo (IBP) (ed), *Rio Pipeline Conference 2015*.